ζ-Crystallin is a bcl-2 mRNA binding protein involved in *bcl-2* overexpression in T-cell acute lymphocytic leukemia

Andrea Lapucci,[*,†,‡,1] Matteo Lulli,[*,†,‡,1] Amedeo Amedei,[‡,§] Laura Papucci,[*,†] Ewa Witort,[*,†] Federico Di Gesualdo,[*,†,‡] Francesco Bertolini,[‖] Gary Brewer,[‡,¶] Angelo Nicolin,[#] Annamaria Bevilacqua,[#] Nicola Schiavone,[*] Dominique Morello,[‡,] Martino Donnini,[*,†,‡,2] and Sergio Capaccioli[*,†,‡,2]**

[*]Department of Experimental Pathology and Oncology and [§]Department of Internal Medicine (Section of Immunology), University of Florence, Florence, Italy; [†]Apoptosis Deregulation in Cancer, Unit of Istituto Toscano Tumori, Florence, Italy; [‡]Phoenix Stem Cell Foundation for Human Life, Florence, Italy; [‖]Division of Clinical Hemato-Oncology, European Institute of Oncology, Milan, Italy; [¶]Department of Molecular Genetics, Microbiology, and Immunology, Robert Wood Johnson Medical School, University of Medicine and Dentistry of New Jersey, Piscataway, New Jersey, USA; [#]Department of Pharmacology, University of Milan, Milan, Italy; and **Centre de Biologie du Développement, Université Paul Sabatier, Toulouse, France

ABSTRACT **The human antiapoptotic *bcl-2* gene has been discovered in t(14;18) B-cell leukemias/lymphomas because of its overexpression caused at a transcriptional control level by the *bcl-2/IgH* fusion gene. We were the first to disclose the post-transcriptional control of *bcl-2* expression mediated by interactions of an adenine + uracil (AU)-rich element (ARE) in the 3′-UTR of *bcl-2* mRNA with AU-binding proteins (AUBPs). Here, we identify and characterize ζ-crystallin as a new *bcl-2* AUBP, whose silencing or overexpression has impact on *bcl-2* mRNA stability. An increased Bcl-2 level observed in normal phytohemagglutinin (PHA)-activated T lymphocytes, acute lymphatic leukemia (ALL) T-cell lines, and T cells of patients with leukemia in comparison with normal non-PHA-activated T lymphocytes was concomitant with an increase in ζ-crystallin level. The specific association of ζ-crystallin with the *bcl-2* ARE was significantly enhanced in T cells of patients with ALL, which accounts for the higher stability of *bcl-2* mRNA and suggests a possible contribution of ζ-crystallin to *bcl-2* overexpression occurring in this leukemia.—Lapucci, A., Lulli, M., Amedei, A., Papucci, L., Witort, E., Di Gesualdo, F., Bertolini, F., Brewer, G., Nicolin, A., Bevilacqua, A., Schiavone, N., Morello, D., Donnini, M., Capaccioli, S. ζ-Crystallin is a bcl-2 mRNA binding protein involved in *bcl-2* overexpression in T-cell acute lymphocytic leukemia. *FASEB J.* 24, 1852–1865 (2010). www.fasebj.org**

Key Words: post-transcriptional control · cancer · ARE-binding protein

Although the human antiapoptotic Bcl-2 protein was discovered by virtue of its overproduction in t(14;18) B-cell leukemias/lymphomas, in most solid and hematological malignancies Bcl-2 is overproduced in the absence of evident chromosomal rearrangements. Graninger *et al.* (1) first reported that the t(14;18) generates a *bcl-2/IgH* fusion gene, in which *bcl-2* expression is increased at a transcriptional level by the potent enhancer located in the *IgH* moiety of the hybrid gene. We then demonstrated that the *bcl-2/IgH* fusion gene also influences *bcl-2* overexpression by acting at a post-transcriptional level: an antisense transcript generated by the *IgH* moiety increased *bcl-2* mRNA stability (2, 3), masking a destabilizing adenine + uracil-rich element [AU-rich element (ARE)] located in the 3′-UTR of *bcl-2* mRNA (4, 5). Furthermore, we showed that the *bcl-2* ARE modulated *bcl-2* expression at a post-transcriptional level in physiological conditions also by interacting with specific ARE-binding proteins (AUBPs), whose pattern underwent modifications during apoptosis in correlation with increased decay of *bcl-2* mRNA (6) and whose activity included either mRNA stabilization or destabilization (7). We identified AUF1 (8) and Bcl-2 itself (9) as two *bcl-2* mRNA destabilizing AUBPs and discovered TINO as a new RNA binding protein endowed with *bcl-2* mRNA destabilizing activity (10). Other *bcl-2* AUBPs, such as nucleolin (11), Ebp1 (12), and HuR (13), as well as microRNAs targeting *bcl-2* mRNA (14, 15), have been reported by others. Most recently, we disclosed the very intriguing overcoming of the Bcl-2 protein, in its destabilizing role of AUBP, on HuR, as its stabilizing counterpart, in modulation of *bcl-2* mRNA turnover (16).

Focusing on human pathology, it is apparent that *bcl-2* overexpression, which occurs in most solid and hematological malignancies in the absence of *bcl-2* gene rear-

[1] These authors contributed equally to this work.

[2] Correspondence: Department of Experimental Pathology and Oncology, Viale G.B. Morgagni, 50, 50134 Florence, Italy. E-mail: S.C., sergio@unifi.it; M.D., martinod@unifi.it

doi: 10.1096/fj.09-140459

0892-6638/10/0024-1852 © FASEB

rangements (17–19), could be due to impaired ARE/AUBP interaction-based *bcl-2* post-transcriptional control. Here, we identify ζ-crystallin as a new *bcl-2* AUBP endowed with *bcl-2* mRNA stabilizing activity and responsible, if overproduced, for enhanced *bcl-2* mRNA stability in T-cell acute lymphocytic leukemia (ALL).

ALLs are the most common childhood cancers, with peak prevalence between the ages of 2 and 5 yr (20, 21). Although more than 80% of pediatric patients with ALL are cured, the current intensive therapeutic regimens have toxic side effects (22) and the prognosis for the 20–30% of pediatric patients who have a relapse or whose ALL is refractory to conventional therapies remains dismal (23). Indeed, relapsed ALL is the fifth most common pediatric malignancy and the first cause of pediatric cancer mortality (24), patients with T-cell ALL being more prone to early initial relapse and inferior outcome than patients with B-cell ALL (25). Based on previous considerations, advances in the understanding of the pathogenesis of ALLs as well as in the identification of the precise molecular events that take place in their genesis suggest that drugs specifically targeting the genetic alterations could revolutionize management of this disease (26). In this scenario, we propose that deregulated ζ-crystallin could be included among these candidate therapeutic targets.

ζ-Crystallin is a highly conserved protein (27) endowed with pleiotropic functions. First discovered as a structural protein in the lens of guinea pigs (28), camelids (29, 30), and tree frogs (31), it was also found in plants (32) and yeast (33). ζ-Crystallin also has oxidoreductase activity (34, 35) and has been identified as a novel NADPH:quinone reductase (36, 37). More recently, Tang and Curthoys (38) and Ibrahim *et al.* (39) identified ζ-crystallin as an RNA-binding protein, able to stabilize rat *glutaminase* mRNA in conditions of metabolic acidosis by binding to a pH response element (pH-RE) in substitution of the destabilizing AUBP, namely AUF1. In addition, Schroeder *et al.* (40) found that ζ-crystallin also stabilized rat *glutamate dehydrogenase* mRNA by binding to peculiar motifs of its 3′-UTR that are highly homologous to the *glutaminase* mRNA pH-RE. Moreover, Fernández *et al.* (41) have recently reported that ζ-crystallin is a highly evolutionarily conserved AUBP, being able, besides functioning as an NADPH-dependent ortho-quinone reductase, to specifically bind to a synthetic A(UUUA) pentameric probe both in humans and in yeast. Last, Porté *et al.* (27) have further characterized the RNA binding properties of ζ-crystallin, demonstrating that NADPH efficiently competed against the A(UUUA) pentameric probe for binding to human ζ-crystallin, which suggests that the NADPH-binding site is involved in the binding of ζ-crystallin to RNA.

MATERIALS AND METHODS

Cell cultures and transfections

The human ALL Jurkat (clone E6–1), ALL MOLT-4, and lymphocytic lymphoma SUP-T1 T-cell lines and the embryonic kidney HEK 293 cell line (European Collection of Cell Cultures, Porton Down, UK), were cultured according to the supplier's maintenance protocols.

For silencing of ζ-*crystallin* by siRNA, Jurkat cells or HEK 293 cells were electrophorated or transfected using Lipofectamine 2000 reagent (Invitrogen, Carlsbad, CA, USA), respectively, with a combination of two siRNAs (Qiagen, Hilden, Germany) specific for the ζ-*crystallin* or one siRNA (Qiagen) specific for the *green fluorescent protein* (*GFP*) (200 nM final concentration). The sequences of ζ-*crystallin* targeted by the siRNAs were: 5′-CAAGCCTACTTACCTTTATAA-3′ and 5′-CAGAGGTACTATTGAAATAAA-3′. The *GFP* sequence targeted by the siRNA was 5′-CGGCAAGCTGACCCTGAAGTTCAT-3′.

For transient transfection of recombinant ζ-crystallin, a 1016-nucleotide segment corresponding to the entire open reading frame of ζ-*crystallin* was PCR-amplified using 5′-GCGAAGCTTATGGCGACTGGACAGAAGTTG-3′ and 5′-GCCTCGAGTAAGAGAAGAATCATTTTACCAGTAGCC-3′ as forward and reverse primers, respectively, and cloned into the *Hind*III and *Xho*I sites of the pQE-TriSystem vector (Qiagen) to obtain the pQE-TriSystem/HIS-Tag CRYZ expression vector. HEK 293 cells (8×10^5) were transfected with 4 μg of pQE-TriSystem/HIS-Tag CRYZ or the empty vector, using Lipofectamine 2000 reagent (Invitrogen), and analyzed for expression after 48 h by immunoblotting, using anti-HIS (C-term) mAb (Invitrogen).

For chimeric reporter assays, a DNA fragment containing the *bcl-2* ARE was cloned into the *Xba*I cloning site at the 3′ end of the *hRlucP* gene coding for *Renilla reniformis* luciferase of the pGL4.71P plasmid to produce the pGL4.71P bcl2 ARE plasmid, as described previously (42). Forty-eight hours after the first ζ-*crystallin* transfection or silencing of HEK293 cells, the aliquots of 2×10^5 cells were plated in 24-well dishes and were cotransfected for the second time with 500 ng of the pGL4.71P or pGLA4.71P bcl2 ARE constructs and 500 ng of the pGL3-P firefly luciferase reporter gene plasmid.

Blood samples and isolation of T lymphocytes

Peripheral blood samples for preparation of $CD3^+$ T lymphocytes were obtained from 40 healthy middle-aged donors of both sexes and from 4 patients with $CD3^+$ ALL. All patients were thoroughly informed about this study and gave written consent for the investigation. The samples were kept small according to the guidelines of the Italian ethics committee. The T lymphocytes were isolated from peripheral blood mononuclear cells, which had been fractionated, cultured, and activated, when required, with 1% v/v phytohemoagglutinin (PHA) (Life Technologies, Inc., Grand Island, NY, USA), as described previously (43). ALL T lymphocytes were isolated as described above and stored at −80°C until use.

Characterization of $CD3^+$ ALL T cells

Leukemia samples were characterized on the basis of their phenotype, and the absence of evident chromosomal rearrangement was ascertained.

Preparation of cytosolic fractions

Cells were pelleted at 100 *g* for 5 min at 4°C, washed with ice-cold PBS, and lysed in 100 μl of cytosolic lysis buffer (10 mM HEPES, 10 mM KCl, 1 mM EDTA, 1 mM EGTA, 1 mM DTT, 1 mM $MgCl_2$, 5% glycerol, 0.25 mM Pefabloc, 2 μM leupeptin, 0.3 μM aprotinin, and 0.1 mM sodium orthovanadate). After incubation on ice for 10 min, cells were lysed with Nonidet P-40 (final concentration 0.25%), vortexed for 10 s, and than centrifuged for 5 min at 16,000 *g*. Cytoplasmic

supernatants were saved as a cytosolic fraction (44). Protein concentrations were determined using the Qubit fluorimeter (Invitrogen).

UV-cross-linking assays

Aliquots of cytoplasmic proteins (~50 μg) from nonactivated or PHA-activated human T lymphocytes or Jurkat cells were incubated in a total volume of 10 μl with the ^{32}P-labeled *bcl-2* ARE probe (10^9 cpm/μg, 5×10^5 cpm) as described previously (6) and analyzed by a Cyclone Storage Phosphor System (PerkinElmer Life and Analytical Sciences, Waltham, MA, USA).

Isoelectrofocusing and bidimensional electrophoresis

Samples, resuspended in the rehydration buffer, were applied to 7-cm immobilized pH gradient strips (pH 3–10 NL; Invitrogen), incubated at room temperature overnight and then focused in a ZOOM IPGRunner Minicell System (Invitrogen), as recommended by the manufacturer. Focused proteins were separated by bidimensional SDS-PAGE on NuPAGE 4–12% Bis-Tris gels (Invitrogen), and the resulting spots were stained with the SilverQuest Silver staining kit (Invitrogen).

Protein identification by mass spectrometry

The gel spot was excised and processed using the Montage in-Gel Digest kit (Millipore, Billerica, MA, USA), according to the manufacturer's instructions. The digested eluate was analyzed by mass spectrometry on an Ultraflex TOF/TOF instrument (Bruker Daltronics, Bremen, Germany), according to the manufacturer's instructions. The resulting mass picks were analyzed by Mascot Peptide Mass Fingerprint software (Matrix Science Ltd., London, UK) and then searched for in the MSDB database (http://www.matrixscience.com/search_form_select.html).

In vitro transcription

Radiolabeled RNA probes were generated by *in vitro* transcription using a MAXIscript T7 kit (Ambion, Austin, TX, USA) and either pCRII/*bcl-2* ARE (10) or the pCRII/*TA* vector (Invitrogen) as a negative control, using plasmids as templates. Transcription reactions were performed for 1 h at 37°C according to the manufacturer's instructions: 100 U of T7 polymerase; 500 μM concentrations each of ATP, CTP, and GTP; 12.5 μM UTP; 200 μCi of [^{32}P]UTP (800 Ci/mmol; Amersham Biosciences, Piscataway, NJ, USA); and 1 μg of plasmid template linearized by digestion with *Sma*I for pCRII/*bcl-2* ARE or *Hind*III for pCRII/*TA* control, in a total volume of 20 μl. Unincorporated nucleotides were removed using the MEGAclear column kit (Ambion). Biotinylated RNA probes were obtained by *in vitro* transcription with the MEGAscript (Ambion). A 20-μl volume of the final reaction contained 2 μl of 10× transcription buffer and 2 μl each of 75 mM ATP, GTP, and UTP. It also contained 1 μl of 75 mM CTP and 7.5 μl of 10 mM biotinylated CTP (Invitrogen), 10 μg of linearized pCRII/*bcl-2* ARE or pCRII/TA templates, and 2 μl of T7 MEGAscript enzyme mix. After an overnight incubation at 37°C, the transcription reaction was stopped by the addition of 2 μl of RNase-free DNase (DNA-free; Ambion); unincorporated nucleotides were removed. The RNA concentration was determined spectrophotometrically at 260 nm.

In vitro translation

ζ-*crystallin* cDNA (Geneservice Ltd., Cambridge, UK) was inserted into the plasmid pCMV-SPORT6 (Image Clone 6067125). On *Mlu*I linearization, the ζ-*crystallin*-harboring plasmid was incubated with the SP6 TNT Coupled Reticulocyte Lysate System (Promega, Madison, WI, USA) in the presence of cold methionine, according to the manufacturer's instructions.

RNA binding assays of *bcl-2* ARE probe to ζ-crystallin in Jurkat cell and PHA-activated T-lymphocyte extracts

RNA binding assays were performed essentially according to Cok *et al.* (44). In brief, cytoplasmic proteins (4 mg/400 μl) were incubated with 120–150 μg of biotinylated RNA probes in the presence of 20 U of Recombinant RNasin Inhibitor (Promega) for 2 h with constant rotation and then were treated with 600 μl of streptavidin-agarose beads (Invitrogen). The mixture was prewashed 3 times in 1 ml of binding buffer (10 mM HEPES, pH 7; 6.5 mM $MgCl_2$; 40 mM KCl; 1 mM DTT; 5% glycerol; and 5 mg/ml heparin), for an additional 2 h with constant rotation. Bound proteins were washed 4 times with 1 ml of binding buffer, eluted from the biotinylated RNA with 200 μl of 1 M NaCl in binding buffer, and collected with the ReadyPrep 2-D Cleanup kit (Bio-Rad Laboratories, Hercules, CA, USA). Samples were then resuspended in 150 μl of rehydration buffer (8 M urea; 0.15 mg/ml; 2% CHAPS; 0.5% carrier ampholytes, pH 7–10; 0.0002% bromphenol blue; and 20 mM DTT). All incubations were performed at room temperature. Results were from either four healthy donors or four inoculations of Jurkat cells.

RNA electromobility shift assay (REMSA)

Mobility shift assays were performed using the radiolabeled *bcl-2* ARE or the *pCRII/TA* riboprobes (6). Samples were analyzed using the Cyclone Storage Phosphor System.

Intracellular localization

Cells (2×10^5) were immobilized onto glass cover slips (15×15 mm), washed twice with 1 ml of cold PBS, and fixed for 20 min in 3.7% paraformaldehyde in PBS. After 3 washes for 2 min with PBS, cells were permeabilized with 1 ml of 0.25% Triton X-100 in PBS for 5 min at room temperature and washed 3 times for 5 min in PBS. All of the following treatments were performed in the dark. After staining of the nuclei with Hoechst 33258 (Sigma-Aldrich, St. Louis, MO, USA) in PBS for 30 min at 37°C, the cells were washed 3 times for 5 min with 1 ml of PBS at room temperature, incubated in 1 ml of blocking buffer (3% bovine serum albumin and 0.1% Triton X-100 in PBS) for 1 h at room temperature, and then incubated overnight at 4°C with the primary rabbit polyclonal anti-ζ-crystallin Ab (1:250) in blocking buffer (kindly provided by J. Samuel Zigler, Jr., National Eye Institute, Bethesda, MD, USA). The following day, the cells were washed 3 times for 15 min in washing buffer (0.1% Triton X-100 in PBS), incubated with the secondary Cy-3 conjugated anti-rabbit antibody (Chemicon International, Inc., Temecula, CA, USA) (1:800) for 60 min at room temperature, and washed 3 times with 1 ml of washing buffer for 5 min at room temperature. They were then dried, mounted onto glass slides, and examined with confocal microscopy using a Nikon Eclipse TE2000-U (Nikon, Tokyo, Japan). Confocal images (1024×768 pixels) were obtained using a ×63 objective lens.

Cytofluorimetric analysis of levels of Bcl-2 and ζ-crystallin proteins

Nonactivated or PHA-activated T lymphocytes and Jurkat cells were stained with anti-CD3 fluorescent mAb (BD, Franklin Lakes, NJ, USA) and then with anti-Bcl-2 mAb (Upstate Biotechnology, Charlottesville, VA, USA) or rabbit polyclonal anti-ζ-crystallin Ab. In brief, 10^6 cells were incubated with the anti-CD3 mAb at +4°C for 30 min, washed with PBS containing 1% bovine serum albumin and 0.1% sodium azide, and then fixed and permeabilized with a permeabilizing solution (BD) for 10 min. Cells were incubated with mouse anti-Bcl-2 or rabbit anti-ζ-crystallin Ab or the isotype control mAb (BD Biosciences Pharmingen, San Diego, CA, USA) at +4°C for 30 min. They were then washed with PBS, which contained 0.5% saponin and 0.1% sodium azide, stained with goat anti-mouse IgG-FITC (BD) or goat anti-rabbit IgG-FITC (Molecular Probes, Eugene, OR, USA) at +4°C for 15 min, and analyzed on a BDLSRII cytofluorimeter using Diva software (BD) with 10^4 events for each sample acquired.

In vivo cross-linking and immunoprecipitation (IP)/RT-PCR

Protein extracts (2 mg) of the Jurkat cell line were cross-linked *in vivo* with formaldehyde (45) and precleared with 30 μl of a 50% slurry of rProtein G-Agarose beads (Invitrogen), 250 mM NaCl, and 400/U RNasin for 3 h at 4°C and then immunoprecipitated with 30 μl of a 50% slurry of rProtein G Agarose beads, anti-ζ-crystallin Ab, or preimmune serum (1:100) and incubated overnight at 4°C. After extensive washes, one-half of the beads were used for immunoblot analysis with the anti-ζ-crystallin Ab. For the IP/RT-PCR, the other half was used for subsequent RNA purification using an RNeasy Kit (Qiagen) and treated with DNA-free. Purified RNA was retro-transcribed by the iScript cDNA Synthesis kit (Bio-Rad Laboratories, Hercules, CA, USA), and cDNA was amplified with primers for *bcl-2*, *glutaminase,* and β-*actin* described below in the Real-Time PCR section.

Immunoblot analysis

The cytoplasmic proteins (50 μg) were separated by NuPAGE 12% Bis-Tris Gel and electroblotted (Trans-Blot Semi-Dry apparatus; Bio-Rad) onto Protran nitrocellulose transfer membranes (Schleicher & Schuell, Dassel, Germany). The following antibodies were used: rabbit-polyclonal ζ-crystallin, AUF1, and β-actin (Santa Cruz Technology, Inc., Santa Cruz, CA, USA) and monoclonal Bcl-2 and α-tubulin (Sigma-Aldrich). The secondary antibodies included goat anti-mouse IRDye 800CW and goat anti-rabbit IRDye 800CW (Li-Cor Biosciences, Lincoln, NE, USA). The protein bands were analyzed by the Odyssey Infrared Imaging System (Li-Cor) using the software for protein quantification.

Real-time PCR

Total RNA was isolated from nonactivated or PHA-activated T lymphocytes, cultured ALL T cells, ALL T cells obtained from patients with leukemia (~5×10^6 cells/sample), and HEK 293 cells with an RNeasy mini kit (Qiagen), treated with RNase-free DNase, and analyzed spectroscopically. One microgram of RNA was retrotranscribed using iScript (Bio-Rad) and amplified with specific primers: For *bcl-2,* forward 5′-TCAGCTATTTACTGCCAAAG-3′ and reverse 5′-GATTTCCAAAGACAGGAG-3′; for *glutaminase,* forward 5′-CCTAGATGGCACCTCCTTTGG-3′ and reverse 5′-TGCTACCTGTCTCCATGGCTTG-3′; for *18S,* forward 5′-CGGCTACCACATCCAAGGAA-3′ and reverse 5′-GCT-

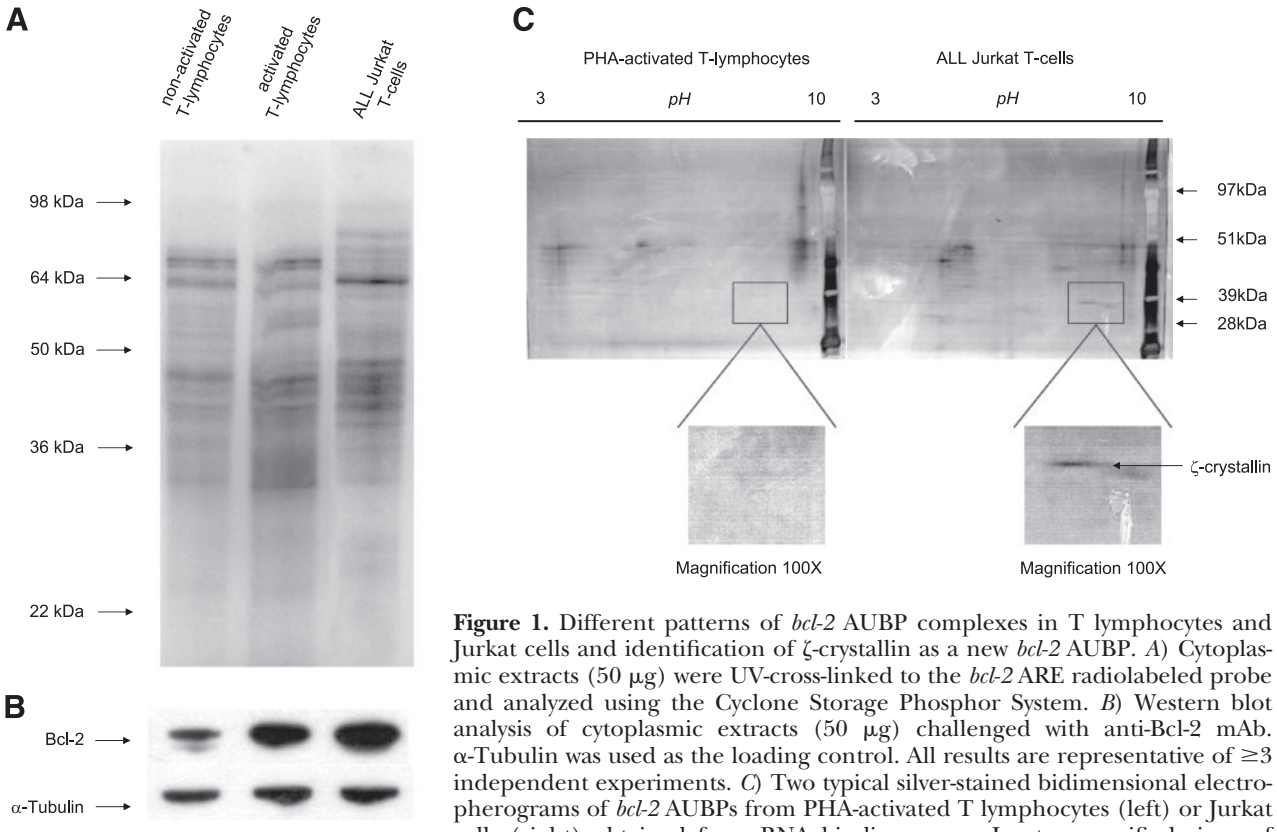

Figure 1. Different patterns of *bcl-2* AUBP complexes in T lymphocytes and Jurkat cells and identification of ζ-crystallin as a new *bcl-2* AUBP. *A*) Cytoplasmic extracts (50 μg) were UV-cross-linked to the *bcl-2* ARE radiolabeled probe and analyzed using the Cyclone Storage Phosphor System. *B*) Western blot analysis of cytoplasmic extracts (50 μg) challenged with anti-Bcl-2 mAb. α-Tubulin was used as the loading control. All results are representative of ≥3 independent experiments. *C*) Two typical silver-stained bidimensional electropherograms of *bcl-2* AUBPs from PHA-activated T lymphocytes (left) or Jurkat cells (right) obtained from RNA binding assays. Insets: magnified views of corresponding boxed areas.

TABLE 1. *Summary of tryptic peptides of human ζ-crystallin protein sequenced by MALDI-TOF mass spectrometry*

ζ-Crystallin protein	Observed mass (*m/z*)	Sequence	Amino acid residues
Peptide 1	1054.575	DLSLLSHGGR	CRYZ: 233-242
Peptide 2	1221.657	VFEFGGPEVLK	CRYZ: 13-23
Peptide 3	1468.791	ESSIIGVTLFSSTK	CRYZ: 263-276
Peptide 4	1527.805	QGAAIGIPYFTAYR	CRYZ: 125-138
Peptide 5	1614.814	VHACGVNPVETYIR	CRYZ: 42-55
Peptide 6	1633.860	IVLQNGAHEVFNHR	CRYZ: 188-201
Peptide 7	2180.131	AGESVLVHGASGGVGLAACQ IAR	CRYZ: 148-170
Peptide 8	2551.260	VFTSSTISGGYAEYALAADH TVYK	CRYZ: 93-116

GGAATTACCGCGGCT-3′; for β-*actin,* forward 5′-GAAACTACCTTCAACTCCATCATG-3′ and reverse 5′-AGGAGGAGCAATGATCTTGATC-3′; for *R. reniformis luciferase,* forward 5′-GTCGAGACCATGCTCCCAAGCA-3′ and reverse 5′-TTGCGGACAATCTGGACGACGT-3′; and for firefly *luciferase,* forward 5′-CTGAATTGGAATCCATCTTGCTCCAACAC-3′ and reverse 5′-TTCGTCCACAAACACAACTCCTCCG-3′. All primers were purchased from Eurofins MWG Operon (Ebersberg, Germany). Real-time PCR assays were performed using the Rotor-Gene 3000 cycler system (Corbett Research, Sydney, NSW, Australia).

mRNA decay assay

Forty-eight hours after ζ-*crystallin* transient transfection or silencing, or 24 h after transient transfection of chimeric reporters, cells were treated with actinomycin D at a final concentration of 5 μg/ml to block transcription and harvested at various time points. Total RNA was extracted, and the real-time PCR assays were performed as described above. The quantification of *bcl-2* mRNA and heterogenous nuclear RNA (hnRNA) for the *bcl-2* mRNA stability assessment was performed by PCR amplification, according to the strategy described by Otake *et al.* (46), using the same primers and amplification conditions. PCR amplification of *18S* rRNA and β-*actin* RNA were used as the normalizer. In the chimeric reporter assay, *R. reniformis* and firefly *luciferase* quantification data were normalized on the expression of the housekeeping gene *18S*, and then the *R. reniformis* data were normalized on transfection efficiency by using firefly *luciferase* mRNA levels. The data from the mRNA decay assays are reported as a percentage of remaining RNA after actinomycin D addition.

Binding of *bcl-2* ARE to ζ-crystallin in cytoplasmic extracts of nonactivated or PHA-activated T lymphocytes, ALL T-cell lines, and ALL T cells from patients with leukemia

bcl-2 ARE radiolabeled probe and cytoplasmic extracts obtained from either nonactivated or PHA-activated T lymphocytes from 4 healthy donors or the 3 ALL T-cell lines or the ALL T lymphocytes from 4 patients with leukemia were prepared as described above. Aliquots of cytoplasmic fractions containing 100 μg of proteins were precleared with rProtein G Agarose beads in cytosolic lysis buffer containing 150 mM KCl. The cytosolic fractions were then incubated for 3.5 h at 4°C with 0.25 nM *bcl-2* ARE and either 2 μg of anti-ζ-crystallin antibody or preimmune serum (control antibody). The immunocomplexes were precipitated with protein G, washed twice with cytosolic lysis buffer, and then analyzed by liquid scintillation. Results are the means ± SE of 3 independent experiments (46). The specificity of binding of our anti-ζ-crystallin antibody was confirmed by the fact that

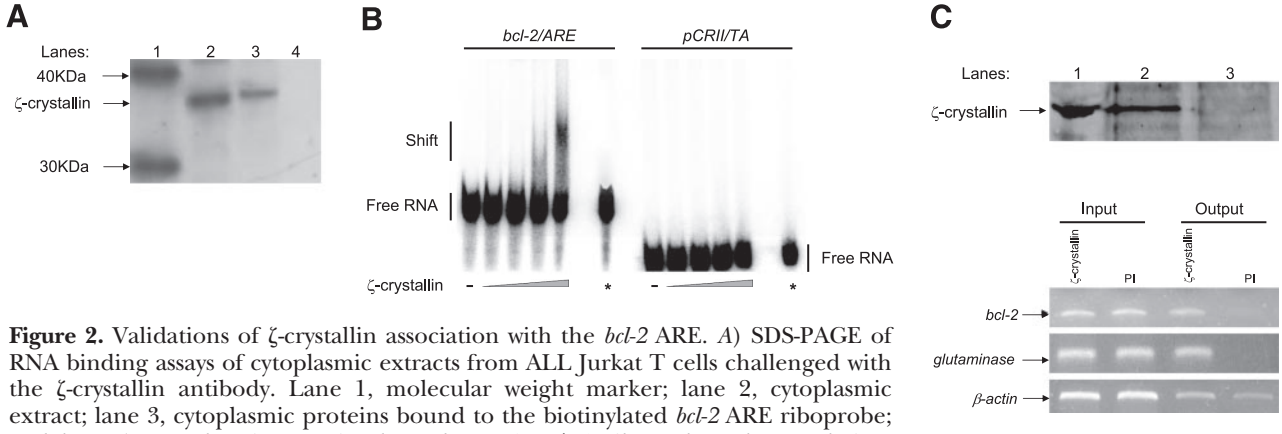

Figure 2. Validations of ζ-crystallin association with the *bcl-2* ARE. *A*) SDS-PAGE of RNA binding assays of cytoplasmic extracts from ALL Jurkat T cells challenged with the ζ-crystallin antibody. Lane 1, molecular weight marker; lane 2, cytoplasmic extract; lane 3, cytoplasmic proteins bound to the biotinylated *bcl-2* ARE riboprobe; and lane 4, cytoplasmic proteins bound to *pCRII/TA* riboprobe. The result is a paradigm of 5 experiments. *B*) REMSA obtained by incubating increasing amounts of *in vitro* synthesized ζ-crystallin with the radiolabeled *bcl-2* ARE (left) or *pCRII/TA* probes (right). Asterisks indicate the maximum volume of a mixture containing the *in vitro* synthesized luciferase and either the *bcl-2* ARE or the *pCRII/TA* probes. The result is a paradigm of 3 independent experiments. *C*) ζ-Crystallin/*bcl-2* mRNA complex in Jurkat cells evaluated by IP/RT-PCR. Immunoblot analyses (above): lane 1, protein extracts; lane 2, immunoprecipitated ζ-crystallin; and lane 3, immunoprecipitation with preimmune serum. Agarose gel electrophoresis (below) shows that the bands corresponding to *bcl-2* and *glutaminase* (as a positive control) mRNAs in the immunoprecipitated complex (output) are restricted to the lane corresponding to the ζ-crystallin antibody. Amplification of the housekeeping gene β-*actin*, bound at low levels with the immunoprecipitated complexes, shows equal loading of immunoprecipitation samples.

>4-fold higher radioactivity was recovered from all immunoprecipitates with the anti-ζ-crystallin antibody compared with those with preimmune serum.

Statistical analysis

Statistical evaluation of the data was performed with a 2-tailed Student's *t* test using STATA 9.0 analysis software (StataCorp LP, College Station, TX, USA). Differences were considered statistically significant when $P \leq 0.05$.

RESULTS

Identification of ζ-crystallin as a new cytoplasmic *bcl-2* AUBP

We used the *bcl-2* overexpressing ALL Jurkat T-cell line *vs.* normal nonactivated or PHA-activated T lymphocytes as the first cellular experimental model. As shown in **Fig. 1,** we analyzed the *bcl-2* AUBP complex pattern, following an RNA-protein UV-cross-linking assay carried out with the synthetic *bcl-2* ARE as probe in 3 cellular cytoplasmic extracts. Western blot analysis of Bcl-2 protein levels was also performed. RNA binding assays using an *bcl-2* ARE-biotin-streptavidin affinity matrix were performed to reveal the binding pattern of single *bcl-2* AUBPs in Jurkat cells and PHA-activated T lymphocytes. Figure 1*A* shows qualitative/quantitative differences in *bcl-2* AUBP complexes, mostly ranging from 25 to 70 kDa, in nonactivated or PHA-activated T lymphocytes and Jurkat cells. Figure 1*B* shows that this phenomenon was accompanied by a significantly higher amount of Bcl-2 protein in the PHA-activated T lymphocytes (6.5 ± 0.7, $P \leq 0.005$) and Jurkat cells (9.3 ± 0.3, $P \leq 0.005$) compared with nonactivated T lymphocytes. To identify specific *bcl-2* AUBPs that un-

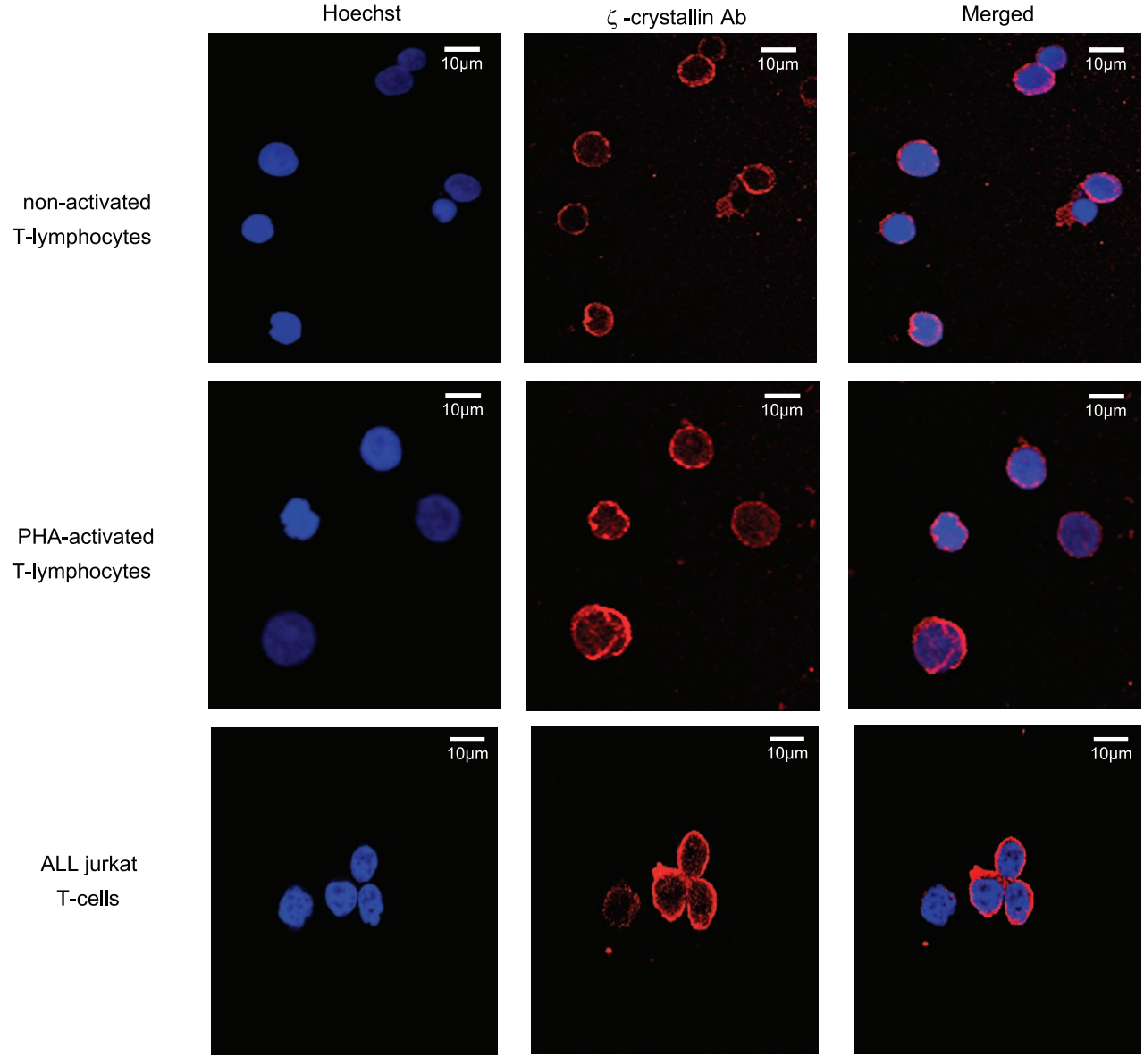

Figure 3. Immunolocalization of ζ-crystallin. Images of nonactivated or PHA-activated T lymphocytes from healthy donor and Jurkat cells obtained through confocal microscopy are shown. Merged images are representative of 6 independent experiments.

dergo quantitative or qualitative changes accounting for *bcl-2* AUBP pattern modifications, the cytoplasmic extracts from PHA-activated T lymphocytes and Jurkat cells were analyzed by RNA binding assays to capture the *bcl-2* AUBPs. The captured proteins were separated by bidimensional SDS-PAGE. Figure 1*C* shows two typical silver-stained bidimensional SDS-PAGE samples of *bcl-2* AUBPs from PHA-activated T lymphocytes (left) or Jurkat cells (right). Among the spots specifically detected in Jurkat cell extracts, we chose the one with an apparent molecular mass of ~35 kDa and pI of ~8–9 for further mass spectrometry analysis. Eight peptides, corresponding to the *m/z* indicated in **Table 1**, were analyzed by Mascot Peptide Mass Fingerprint software in the MSDB database. This resulted in a match with the amino acid sequence of the human ζ-crystallin/NADPH:quinone reductase (*ζ-crystallin* gene; GenBank accession number NM_001889). Sequence analysis by matrix-assisted laser desorption ionization (MALDI)-time of flight (TOF)/TOF of two peptides confirmed the identity of ζ-crystallin (data not shown).

The association of ζ-crystallin with the *bcl-2* ARE was evaluated both *in vitro* and *in vivo* (**Fig. 2**). First, we isolated the AUBPs bound to the biotin/streptavidin conjugated *bcl-2* ARE or *pCRII/TA* (negative control) probes using RNA binding assays and confirmed the presence of ζ-crystallin as a 37- to 38-kDa protein exclusively bound to the *bcl-2* ARE probe (Fig. 2*A*). Then we analyzed the ζ-crystallin binding to the *bcl-2* ARE by REMSA *in vitro*. It clearly demonstrated the shift of the *bcl-2* ARE but not the *pCRII/TA* probe by ζ-crystallin in a dose-dependent manner (Fig. 2*B*). Next, the association of ζ-crystallin with the *bcl-2* ARE was validated *in vivo* by IP/RT-PCR experiments performed with protein extracts from Jurkat cells using a ζ-crystallin antibody or preimmune serum. RT-PCR analysis of ζ-crystallin/RNA immunocomplexes detected coprecipitation of *bcl-2* mRNA with ζ-crystallin protein (Fig. 2*C*).

The cellular localization of ζ-crystallin by confocal immunohistochemistry clearly indicated that ζ-crystallin is a cytoplasmic protein both in nonactivated or PHA-activated T lymphocytes and Jurkat cells (**Fig. 3**).

ζ-Crystallin increases in PHA-activated T lymphocytes to reach levels comparable to those of ALL T-cell lines compared with nonactivated T lymphocytes and correlates with Bcl-2 protein levels

Besides Jurkat, two other *bcl-2*-overexpressing ALL T-cell lines, MOLT-4 and SUP-T1, were included in the analysis of ζ-crystallin expression (**Fig. 4*A***). PHA-activated T lymphocytes displayed higher levels of ζ-crystallin compared with nonactivated T lymphocytes and reached levels similar to those observed in the 3 ALL T-cell lines. Moreover, the enhancement of Bcl-2 protein levels induced by PHA activation was

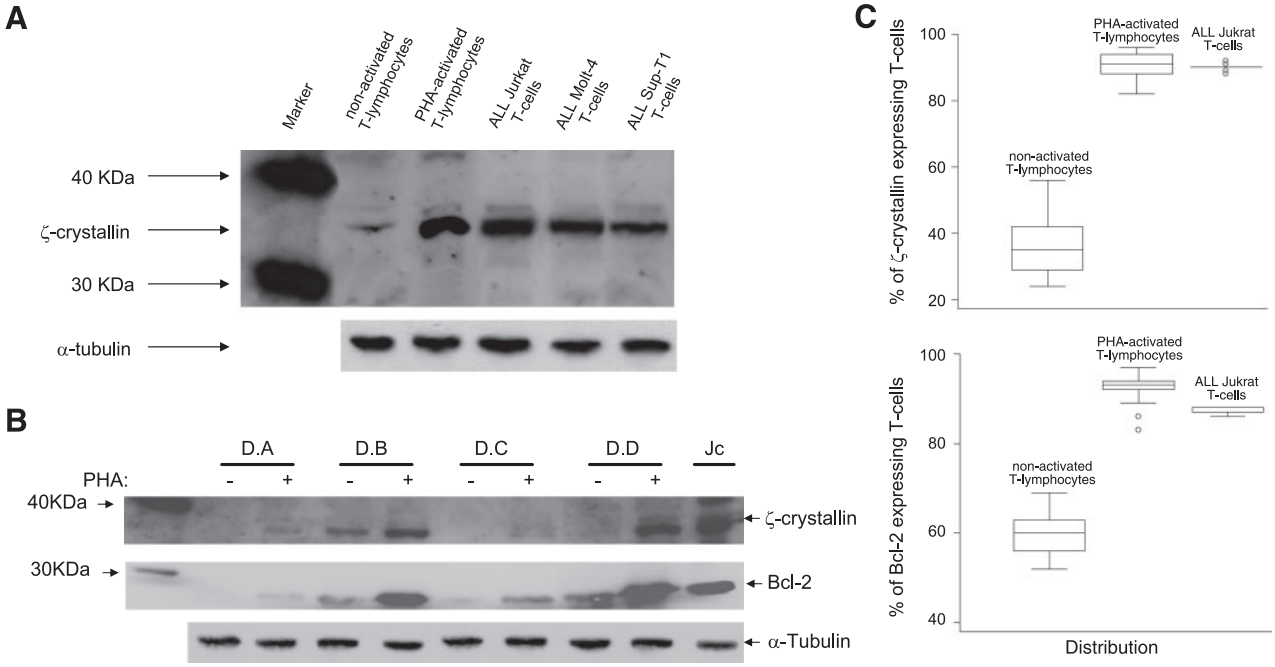

Figure 4. ζ-Crystallin and Bcl-2 levels in nonactivated or PHA-activated T lymphocytes and in ALL T-cell lines. *A*) ζ-Crystallin immunoblot of cytoplasmic extracts from nonactivated or PHA-activated T lymphocytes derived from a healthy donor and ALL T-cell lines (Jurkat, MOLT-4, and SUP-T1). *B*) ζ-Crystallin and Bcl-2 immunoblots of cytoplasmic extracts of nonactivated (−) or PHA-activated (+) T lymphocytes derived from 4 representative healthy donors (D.A to D.D) and from Jurkat cells (Jc). α-Tubulin served as an internal control. *C*) Box and whisker graphs showing the percentage of ζ-crystallin-expressing (top) and Bcl-2-expressing cells (bottom) among nonactivated or PHA-activated T lymphocytes and Jurkat cells, evaluated by FACS analysis. Boxes contain the middle 50% of the data. Horizontal bars indicate means ± SE of 30 observations ($P \leq 0.00005$ for PHA-activated T lymphocytes or Jurkat cells *vs.* nonactivated T lymphocytes; Student's *t* test).

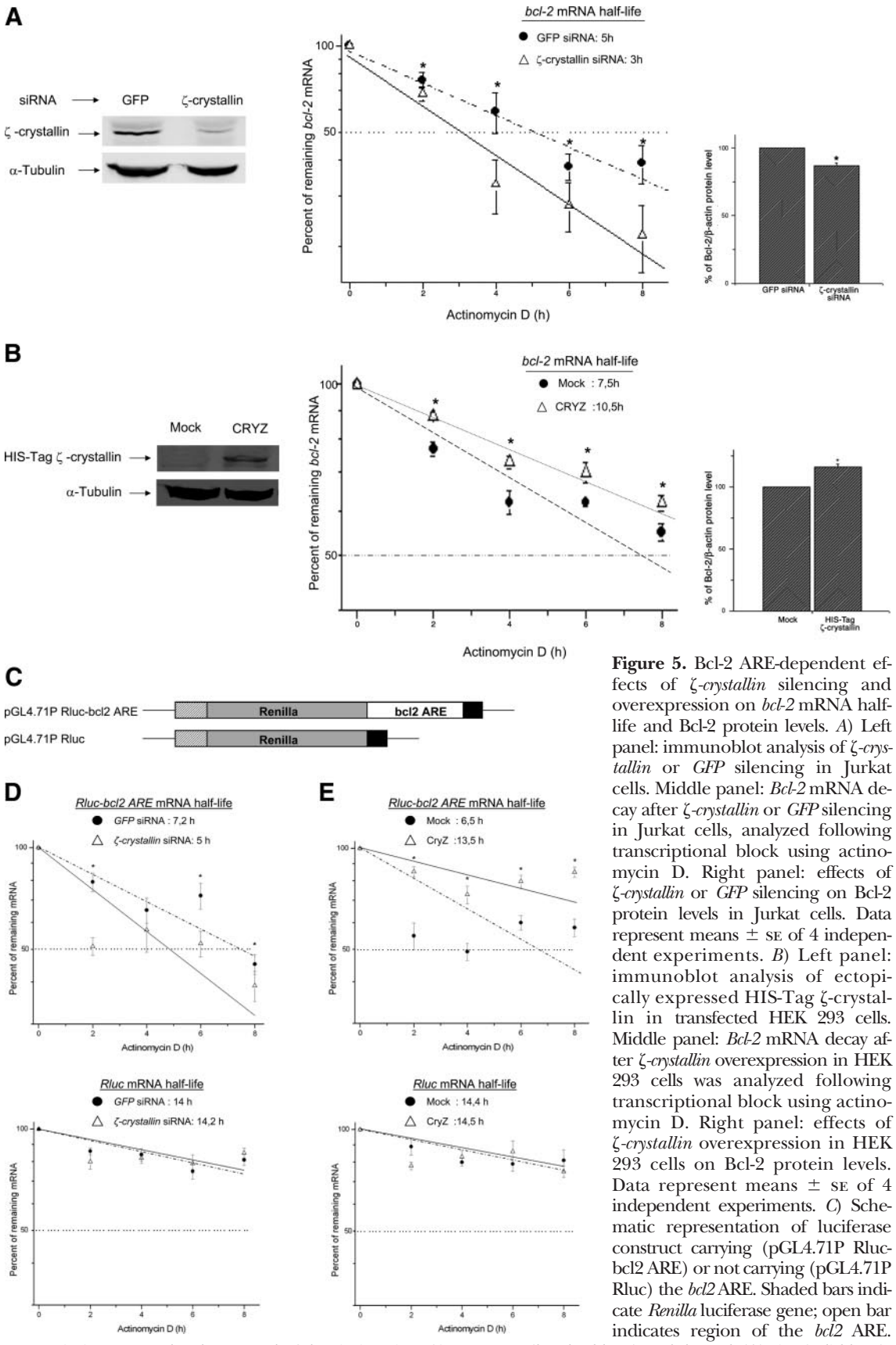

Figure 5. Bcl-2 ARE-dependent effects of ζ-*crystallin* silencing and overexpression on *bcl-2* mRNA half-life and Bcl-2 protein levels. *A*) Left panel: immunoblot analysis of ζ-*crystallin* or *GFP* silencing in Jurkat cells. Middle panel: *Bcl-2* mRNA decay after ζ-*crystallin* or *GFP* silencing in Jurkat cells, analyzed following transcriptional block using actinomycin D. Right panel: effects of ζ-*crystallin* or *GFP* silencing on Bcl-2 protein levels in Jurkat cells. Data represent means ± SE of 4 independent experiments. *B*) Left panel: immunoblot analysis of ectopically expressed HIS-Tag ζ-crystallin in transfected HEK 293 cells. Middle panel: *Bcl-2* mRNA decay after ζ-*crystallin* overexpression in HEK 293 cells was analyzed following transcriptional block using actinomycin D. Right panel: effects of ζ-*crystallin* overexpression in HEK 293 cells on Bcl-2 protein levels. Data represent means ± SE of 4 independent experiments. *C*) Schematic representation of luciferase construct carrying (pGL4.71P Rluc-bcl2 ARE) or not carrying (pGL4.71P Rluc) the *bcl2* ARE. Shaded bars indicate *Renilla* luciferase gene; open bar indicates region of the *bcl2* ARE. Transcription was under the control of the simian virus 40 promoter (hatched bars) and the poly(A) site (solid bars). *D*) *Rluc-bcl-2 ARE* (top) or *Rluc* (bottom) mRNA decay after ζ-*crystallin* or *GFP* silencing in HEK 293 cells, analyzed after transcriptional block using actinomycin D. *E*) *Rluc-bcl-2 ARE* (top) or *Rluc* (bottom) mRNA decay after ζ-*crystallin* overexpression in HEK 293 cells, analyzed following transcriptional block using actinomycin D. Data are means ± SE of 3 independent experiments. Horizontal dotted line in each graph indicates mRNA half-life. *$P \leq 0.005$.

concomitant with that of ζ-crystallin and reached the same values as those observed in Jurkat cells (Fig. 2*B*). Results of flow cytometry showed that, analogically, the PHA activation concomitantly increased the percentage of ζ-crystallin and Bcl-2-expressing cells compared with nonactivated T lymphocytes (from 36.2±8.41 to 90.3±3.74% for ζ-crystallin and from 59.6±5.00 to 92.7±2.89% for Bcl-2, $P \leq 0.00005$), reaching the constitutive levels of Jurkat cells (90.0±0.9% for the ζ-crystallin and 87.26±0.69% for Bcl-2 ($P \leq 0.00005$) (Fig. 2*C*). These data indicate a correlation between Bcl-2 and ζ-crystallin protein levels.

ζ-Crystallin is endowed with *bcl-2* mRNA stabilizing activity in a *bcl-2* ARE-dependent manner

The hypothesis that ζ-crystallin controls *bcl-2* expression at the post-transcriptional level by affecting *bcl-2* mRNA stability was confirmed by a causal relationship between the two events (**Fig. 5**). First, we verified the possible consequence of ζ-*crystallin* silencing on *bcl-2* mRNA decay. The silencing of ζ-*crystallin*, but not of *GFP*, with specific siRNAs in Jurkat cells led to a dramatic reduction (more than 75%) (Fig. 5*A*) in the ζ-crystallin protein level, concomitant with a significant decrease in the *bcl-2* mRNA half-life (from 5 to 3 h, $P \leq 0.005$) and Bcl-2 protein level (13±0.52%, $P \leq 0.005$). Second, we tested the impact of ζ-crystallin overexpression in HEK 293 cells transfected with HIS-Tag ζ-crystallin on *bcl-2* mRNA stability (Fig. 5*B*) and noted the significant increase in the *bcl-2* mRNA half-life (from 7.5 to 10.5 h, $P \leq 0.005$) and Bcl-2 protein level (12±0.67%, $P \leq 0.005$). The difference in the basal *bcl-2* mRNA half-life between the Jurkat (5 h) and HEK 293 (7.5 h) cells was fully justified by the different gene expression pattern that characterizes the two different cell types.

Finally, two symmetrical clear-cut affirmations assured that the stabilizing effect of ζ-crystallin on *bcl-2* mRNA is *bcl-2* ARE-dependent and excluded the possibility that the alteration in *bcl-2* mRNA stability is consequent to the toxicity of ζ-crystallin exogenous modulations. The *bcl-2* ARE regulative effects on mRNA stability were studied using the *bcl-2* ARE-luciferase reporter constructs (Fig. 5*C*). Figure 5*D* shows that silencing of ζ-*crystallin*, but not of *GFP*, in HEK 293 cells reduced the *bcl-2* ARE-bearing *Renilla* luciferase reporter (*Rluc-bcl-2 ARE*) mRNA from 7.2 to 5 h ($P \leq 0.005$). Symmetrically, Fig. 5*E* shows that ζ-crystallin overexpression in HEK 293 cells increased the *Rluc-bcl-2 ARE* mRNA half-life from 6.5 to 13.5 h ($P \leq 0.005$). As expected, ζ-crystallin exogenous modulation did not have any effect on the half-life of *hRluc* devoid of *bcl-2* ARE, used as a negative control. Moreover, in the same experimental model we observed a significant decrease (60±4%, $P \leq 0.0005$) or increase (115±3.4%, $P \leq 0.0005$) of *Rluc-bcl-2 ARE* with respect to *Rluc* mRNA steady states by ζ-*crystallin* silencing or overexpression, respectively. The same modulative effects were also observed in a luciferase reporter protein expression assay (data not show).

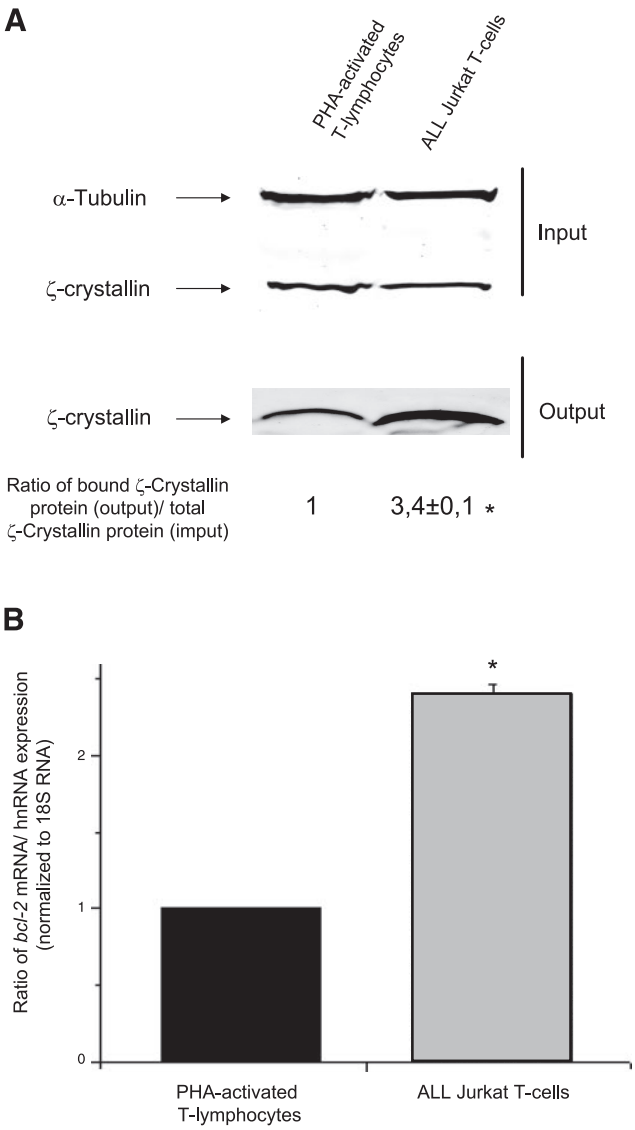

Figure 6. Differential association of ζ-crystallin with the *bcl-2* ARE probe in PHA-activated T lymphocytes and Jurkat cells and relative levels of *bcl-2* mRNA decay. *A*) ζ-Crystallin immunoblots of cytoplasmic extracts from PHA-activated T lymphocytes and Jurkat cells, before (input) and after (output) RNA binding assays using the *bcl-2* ARE probe. α-Tubulin was used as the input protein loading control. Quantitative data of the relative binding of ζ-crystallin to the *bcl-2* ARE probe are reported as the ratio of bound ζ-crystallin (output) to total ζ-crystallin (input) expressed as means ± SE of 4 experiments. *B*) Ratio of the *bcl-2* mRNA/hnRNA levels in PHA-activated T lymphocytes and Jurkat cells determined by real-time PCR and normalized to the *18S* rRNA. Results are means ± SE of 4 experiments. $*P \leq 0.001$.

Association of ζ-crystallin with the *bcl-2* ARE is stronger in Jurkat cells than in PHA-activated T lymphocytes and results in increased *bcl-2* mRNA stability

Although ζ-crystallin protein levels in Jurkat cells are comparable to those of PHA-activated T lymphocytes from healthy donors (Fig. 4), detection of the *bcl-2* ARE-associated ζ-crystallin by silver staining was re-

stricted to Jurkat cells (Fig. 1*C*). This prompted us to investigate the association of ζ-crystallin with *bcl-2* ARE in leukemia cells compared with that in normal lymphocytes. The levels of ζ-crystallin in cytoplasmic extracts were compared before (input) and after (output) RNA binding to a biotinylated *bcl-2* ARE probe (**Fig. 6*A***). Association in Jurkat cells was 3.4-fold greater than in the PHA-activated T lymphocytes ($P \leq 0.001$). This is in keeping with the 2.4-fold increase in *bcl-2* mRNA stability (Fig. 6*B*), measured as the ratio of *bcl-2* mRNA and *bcl-2* hnRNA expression (37) scored by real-time PCR.

Bcl-2 overexpression in ALL T cells from patients with leukemia is accompanied by the stabilization of *bcl-2* mRNA consequent to increased association of ζ-crystallin with its ARE

We then evaluated the possibility that the increased association of ζ-crystallin with *bcl-2* ARE observed in cultured Jurkat cells also occurs in spontaneous T-cell ALL and possibly accounts for the pathogenetic mechanism of this malignancy. We extended our analyses to ALL T cells obtained from four patients, compared with nonactivated or PHA-activated T lymphocytes (**Fig. 7**). As shown in Fig. 7*A*, the levels of Bcl-2 protein (above) in ALL T cells from patients were ~9-fold higher than those in nonactivated T lymphocytes but also, although to a much lower extent, were significantly higher than those in PHA-activated T lymphocytes, which confirmed in spontaneous leukemias the trend observed in the 3 ALL cultured T-cell lines. On the other hand (below), ζ-crystallin levels in ALL T cells from patients were ~5-fold higher than those in nonactivated T lymphocytes but did not differ from those scored in PHA-activated T lymphocytes.

Although the ratios of Bcl-2 and ζ-crystallin to β-actin protein levels plotted in Fig. 7*B* ($r=0.769$, $P \leq 0.001$) indicated that they were significantly correlated, it is unclear why ALL T cells from patients had higher levels of Bcl-2 compared with PHA-activated T lymphocytes

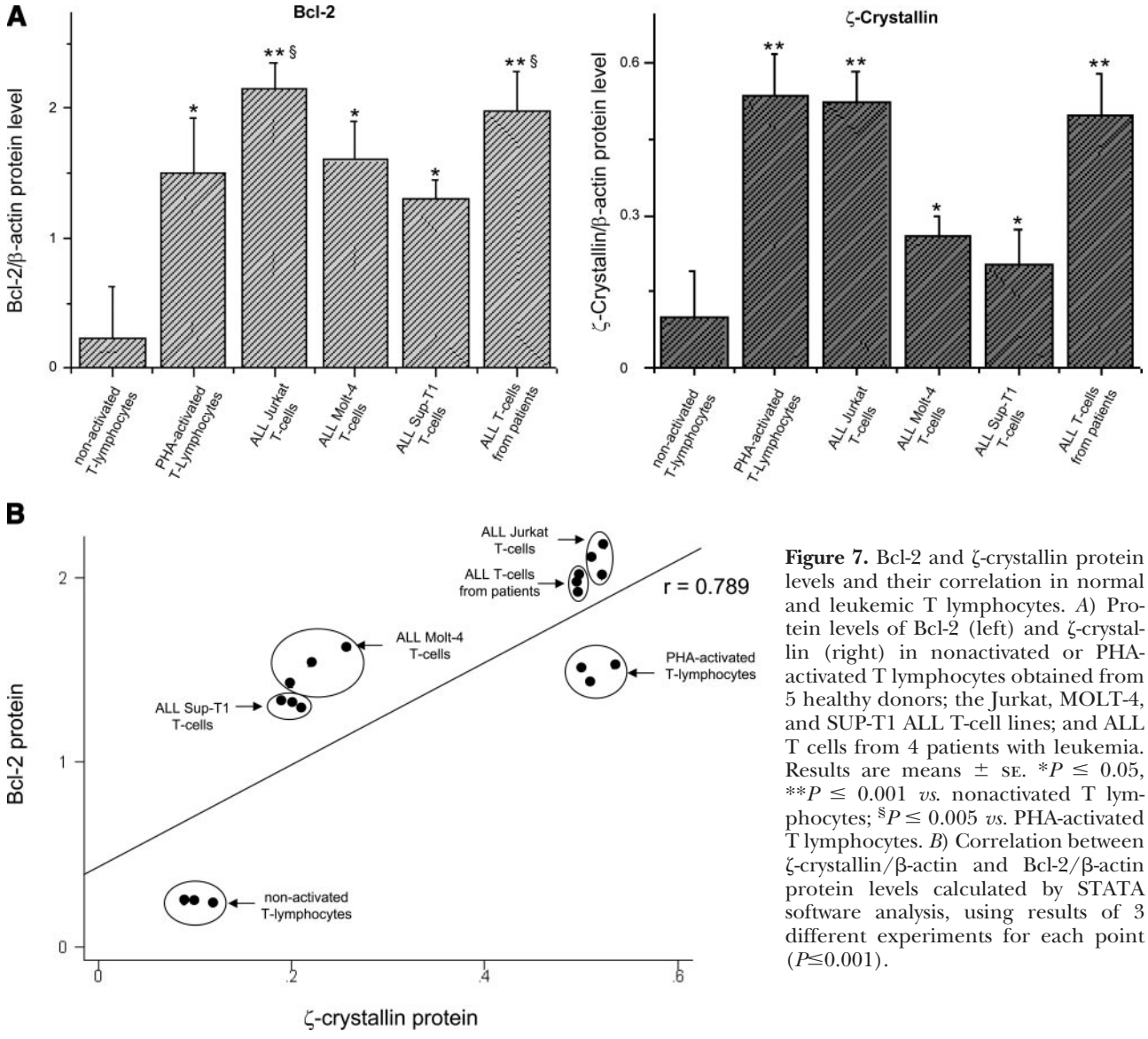

Figure 7. Bcl-2 and ζ-crystallin protein levels and their correlation in normal and leukemic T lymphocytes. *A*) Protein levels of Bcl-2 (left) and ζ-crystallin (right) in nonactivated or PHA-activated T lymphocytes obtained from 5 healthy donors; the Jurkat, MOLT-4, and SUP-T1 ALL T-cell lines; and ALL T cells from 4 patients with leukemia. Results are means ± SE. $^{*}P \leq 0.05$, $^{**}P \leq 0.001$ *vs.* nonactivated T lymphocytes; $^{\S}P \leq 0.005$ *vs.* PHA-activated T lymphocytes. *B*) Correlation between ζ-crystallin/β-actin and Bcl-2/β-actin protein levels calculated by STATA software analysis, using results of 3 different experiments for each point ($P \leq 0.001$).

despite having the same levels of ζ-crystallin. A possible explanation for this discrepancy was the lower decay of *bcl-2* mRNA in ALL T cells compared with that in normal and both nonactivated and PHA-activated T lymphocytes, already observed in Jurkat cells (Fig. 6*B*). Results of *bcl-2* mRNA decay shown in **Fig. 8*A***, indicating that the ratio of *bcl-2* mRNA to hnRNA levels in ALL T cells from patients was 3.3 ± 0.01-fold higher than that in PHA-activated T lymphocytes ($P \leq 0.001$), confirmed this hypothesis. In turn, an obvious explanation for this evidence could be the stronger association of ζ-crystallin with the *bcl-2* ARE in ALL T cells. This hypothesis was confirmed by the results of RNA binding assays obtained by using a *bcl-2* ARE radiolabeled probe (Fig. 8*B*), indicating that the association of ζ-crystallin with the probe was 2.3-fold higher in extracts obtained from patients with leukemia (439±16 cpm) than in those obtained in normal PHA-activated T lymphocytes (195±16 cpm).

On the whole, our results indicate that the increased level of ζ-crystallin as well as its stronger association with the *bcl-2* ARE in ALL T cells enhances *bcl-2* mRNA stability and may thereby be involved in *bcl-2* overexpression typical of this malignancy.

DISCUSSION

T-cell ALL is a rare but aggressive malignancy that represents 15% of childhood and 25% of adult ALLs (47). A high percentage of T-cell ALLs do not contain obvious chromosomal translocations (48). Nevertheless, cytogenetically cryptic abnormalities that can lead either to oncogene activation or to the loss of tumor suppressor genes have been frequently described (49). One of these abnormalities involves *bcl-2*, which plays a fundamental role during T lymphocyte development (50) and whose overexpression in T-cell ALLs contributes to the accumulation of apoptosis-defective chemoresistant T lymphocytes (18, 51–53). Nevertheless, the mechanism underlying *bcl-2* overexpression in T-cell ALLs has not yet been fully unraveled.

We have discovered that *bcl-2* expression can also be controlled at a post-transcriptional level through cooperation between an ARE located in the 3′-UTR of its mRNA (4) and multiple ARE-binding proteins, whose expression pattern undergoes modifications during apoptosis (6). We also identified 3 regulatory *bcl-2* AUBPs: AUF1, Bcl-2 itself, and Tino (8–10). Nucleolin and Ebp1 have been added to the family of *bcl-2* AUBPs by others and have been demonstrated to be involved in *bcl-2* overexpression in the acute promyelocytic leukemia HL-60 cell line and B-cell chronic lymphocytic leukemias (CLLs) (11, 12, 46). Recently, Cimmino *et al.* (14) demonstrated that two microRNAs, miR-15 and miR-16, also bind to and destabilize *bcl-2* mRNA and are responsible, if deleted, for the onset of CLL.

Here, we used 3 leukemia T-cell lines characterized by high Bcl-2 levels in the absence of obvious *bcl-2* gene rearrangements (54) to shed further light on *bcl-2* post-transcriptional control and its role in leukemias/lymphomas. We first revealed quantitative and qualitative differences in cytoplasmic *bcl-2* AUBP complexes from Jurkat cells compared with nonactivated or PHA-activated T lymphocytes from healthy donors. Bidimensional electrophoresis of *bcl-2* AUBPs from PHA-activated T lymphocytes and Jurkat cells confirmed differential patterns of *bcl-2* AUBPs. We hypothesized that *bcl-2* overexpression is caused by alterations of specific AUBPs.

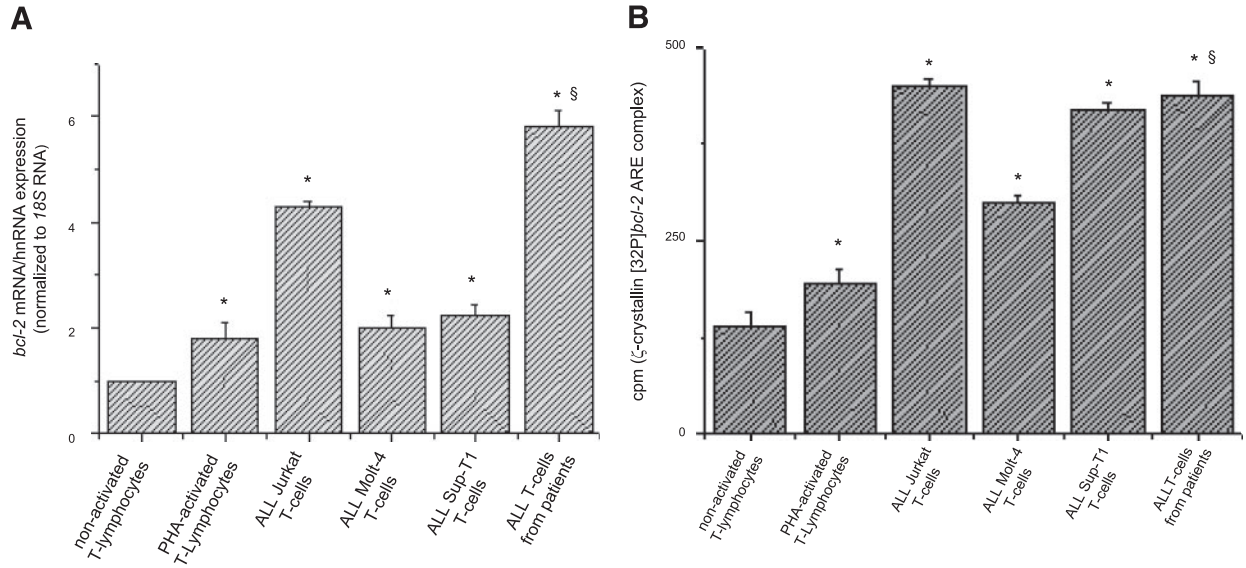

Figure 8. Bcl-2 decay and differential association of ζ-crystallin with the *bcl-2* ARE probe in our T-cell types. *A*) Ratio of *bcl-2* mRNA/hnRNA levels obtained from the ALL T cells of a patient with leukemia and all our T-cell types indicated in Fig. 7, determined by real-time PCR and normalized to the *18S* rRNA. Results are means ± SE of 4 experiments. $*P \leq 0.001$ *vs.* nonactivated T lymphocytes; $^{\S}P \leq 0.001$ *vs.* PHA-activated T lymphocytes. *B*) Counts per minute of ^{32}P-labeled *bcl-2* ARE-ζ-crystallin complexes recovered after ζ-crystallin immunoprecipitation. Columns represent means ± SE of 3 independent experiments. $*P \leq 0.005$ *vs.* nonactivated T lymphocytes; $^{\S}P \leq 0.001$ *vs.* PHA-activated T lymphocytes.

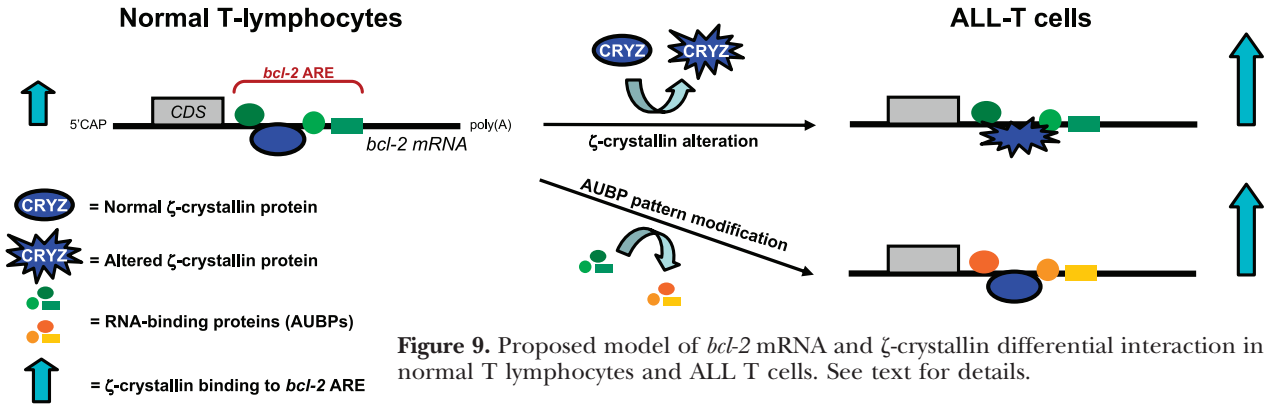

Figure 9. Proposed model of *bcl-2* mRNA and ζ-crystallin differential interaction in normal T lymphocytes and ALL T cells. See text for details.

Among the differentially expressed proteins, we identified the ζ-crystallin/NADPH:quinone reductase as a new *bcl-2* AUBP. The presence of ζ-crystallin in a ribonucleoprotein complex containing *bcl-2* ARE was confirmed both *in vitro* by RNA binding and REMSA assays and *in vivo* by IP/RT-PCR. Our immunolocalization analyses ascertained that ζ-crystallin was an exclusively cytoplasmic protein. Next, we explored its impact on *bcl-2* expression. Both negative and positive modulation of expression in Jurkat cells and HEK 293 cells revealed that ζ-crystallin is endowed with *bcl-2* ARE dependent-stabilizing activity on *bcl-2* mRNA. Although levels of ζ-crystallin in PHA-activated T lymphocytes are comparable, its association with the *bcl-2* ARE in leukemia cells is stronger than that in normal T lymphocytes. This accounts for the higher *bcl-2* mRNA stability in T-cell ALLs, which results in the increased Bcl-2 protein level. Similarly, the binding to *bcl-2* ARE of another *bcl-2* AUBP, nucleolin, has been reported to be ~5-fold greater in CLL B cells than in normal B lymphocytes (46). The authors explained this result as being consequent to the 6.5-fold greater cytoplasmic level of nucleolin in CLL B cells, which indicates that *bcl-2* mRNA binding of nucleolin undergoes quantitative alterations in these cells. In our system, the ζ-crystallin association with the *bcl-2* ARE was much greater in ALL T cells from patients with leukemia and in the 3 leukemia T-cell lines than in normal nonactivated or PHA-activated T lymphocytes. However, cytoplasmic levels of ζ-crystallin did not differ in normal PHA-activated T lymphocytes and leukemia T cells, indicating that the varying concentration-independent binding of ζ-crystallin to the *bcl-2* ARE in leukemia T cells might depend on other parameters. Therefore, we propose a schematic model to explain the differential interaction of ζ-crystallin with the *bcl-2* ARE in normal T lymphocytes and ALL T cells (**Fig. 9**). In this model, we propose two alternative mechanisms. In the first, qualitative modifications undergone by ζ-crystallin in ALL T cells respect to normal T lymphocytes increase its binding to *bcl-2* mRNA, consequently altering the *bcl-2* AUBP pattern. In the second, modifications of the *bcl-2* AUBP pattern in ALL T cells could favor the ζ-crystallin interaction with the *bcl-2* ARE.

Other AUBPs, including AUF-1, Tino, nucleolin, HuR, and Bcl-2 itself and two microRNAs, are known to bind to *bcl-2* mRNA to modulate its turnover in different cell types and to be involved in *bcl-2* overexpression in human leukemias (8–14, 16). There is also the possibility that their simultaneous expression in one cell type in different physiological conditions is not an axiom, implying that their interactions and possible deregulation pathways in human diseases are highly complex. Furthermore, because the binding site of one *bcl-2* AUBP could either overlap or not overlap that of another, possible interactions among different AUBPs compared with the *bcl-2 ARE* and their resulting effects on *bcl-2* mRNA fate are unpredictable *a priori*.

The involvement of ζ-crystallin in *bcl-2* overexpression in ALL T cells might constitute a significant molecular pathogenetic mechanism of the disease. The possibility that ζ-crystallin contributing to *bcl-2* mRNA stabilization observed in T-cell ALLs could also occur in other hematological malignancies or even in solid tumors and its relationships with other AUBPs in *bcl-2* post-transcriptional control are now under investigation in our laboratory. FJ

The authors thank Professors Vieri Boddi and Riccardo Caldini for help with the statistical analysis, Dr. J. Samuel Zigler, Jr. (National Eye Institute, Bethesda, MD, USA) for the contribution of the anti-ζ-crystallin antibody, and Professor Mary Forrest and Dr. Carolyn Demsey for accurate editing of the article. This work was supported by grants from Programmi di Ricerca di Interesse Nazionale (to S.C. and A.N.), the Associazione Italiana per la Ricerca sul Cancro (to S.C.), the Ente Cassa di Risparmio di Firenze (to S.C.), the Fondazione Cassa di Risparmio di Lucca (to S.C.), and the U.S. National Institutes of Health (R01 CA052443 to G.B.).

REFERENCES

1. Graninger, W. B., Seto, M., Boutain, B., Goldman, P., and Korsmeyer, S. J. (1987) Expression of Bcl-2 and Bcl-2-Ig fusion transcripts in normal and neoplastic cells. *J. Clin. Invest.* **80,** 1512–1515
2. Capaccioli, S., Quattrone, A., Schiavone, N., Calastretti, A., Copreni, E., Bevilacqua, A., Canti, G., Gong, L., Morelli, S., and Nicolin, A. (1996) A bcl-2/IgH antisense transcript deregulates bcl-2 gene expression in human follicular lymphoma t(14;18) cell lines. *Oncogene* **13,** 105–115
3. Morelli, S., Delia, D., Capaccioli, S., Quattrone, A., Schiavone, N., Bevilacqua, A., Tomasini, S., and Nicolin, A. (1997) The

antisense bcl-2-IgH transcript is an optimal target for synthetic oligonucleotides. *Proc. Natl. Acad. Sci. U. S. A.* **94,** 8150–8155
4. Schiavone, N., Rosini, P., Quattrone, A., Donnini, M., Lapucci, A., Citti, L., Bevilacqua, A., Nicolin, A., and Capaccioli, S. (2000) A conserved AU-rich element in the 3′ untranslated region of bcl-2 mRNA is endowed with destabilizing function that is involved in bcl-2 down-regulation during apoptosis. *FASEB J.* **4,** 174–184
5. Bevilacqua, A., Ceriani, M. C., Capaccioli, S., and Nicolin, A. (2003) Post-transcriptional regulation of gene expression by degradation of messenger RNAs. *J. Cell. Physiol.* **195,** 356–372
6. Donnini, M., Lapucci, A., Papucci, L., Witort, E., Tempestini, A., Brewer, G., Bevilacqua, A., Nicolin, Capaccioli, S., and Schiavone, N. (2001) Apoptosis is associated with early modifications of bcl-2 mRNA AU-binding proteins. *Biochem. Biophys. Res. Commun.* **287,** 1063–1069
7. Barreau, C., Paillard, L., and Osborne, H. O. (2006) AU-rich elements and associated factors: are there unifying principles? *Nucleic Acids Res.* **33,** 7138–7150
8. Lapucci, A., Donnini, M., Papucci, L., Witort, E., Tempestini, A., Bevilacqua, A., Nicolin, A., Brewer, G., Schiavone, N., and Capaccioli, S. (2002) AUF1 is a bcl-2 ARE-binding protein involved in bcl-2 mRNA destabilization during apoptosis. *J. Biol. Chem.* **277,** 16139–16146
9. Bevilacqua, A., Ceriani, M. C., Canti, G., Asnaghi, L., Gherzi, R., Brewer, G., Papucci, L., Schiavone, N., Capaccioli, S., and Nicolin, A. (2003) Bcl-2 protein is required for the ARE-dependent degradation of its own messenger. *J. Biol. Chem.* **278,** 23451–23459
10. Donnini, M., Lapucci, A., Papucci, L., Witort, E., Jacquier, A., Brewer, G., Nicolin, A., Capaccioli, S., and Schiavone, N. (2004) Identification of Tino: a new evolutionarily conserved bcl-2 AU-rich element RNA binding protein. *J. Biol. Chem.* **279,** 20154–20166
11. Sengupta, T. K., Bandyopadhyay, S., Fernandes, D. J., and Spicer, E. K. (2004) Identification of nucleolin as an AU-rich element binding protein involved in bcl-2 mRNA stabilization. *J. Biol. Chem.* **279,** 10855–10863
12. Bose, S. K., Sengupta, T. K., Bandyopadhyay, S., and Spicer, E. K. (2006) Identification of Ebp1 as a component of cytoplasmic bcl-2 mRNP (messenger ribonucleoprotein particle) complexes. *Biochem. J.* **96,** 99–107
13. Ishimaru, D., Ramalingam, S., Sengupta, T. K., Bandyopadhyay, S., Dellis, S., Tholanikunnel, B. G., Fernandes, D. J., and Spicer, E. K. (2009) Regulation of Bcl-2 expression by HuR in HL60 leukemia cells and A431 carcinoma cells. *Mol. Cancer Res.* **7,** 1354–1366
14. Cimmino, A., Calin, G. A., Fabbri, M., Iorio, M. V., Ferracin, M., Shimizu, M., Wojcik, S. E., Aqeilan, R. I., Zupo, S., Dono, M., Rassenti, L., Alder, H., Volinia, S., Liu, C. G., Kipps, T. J., Negrini, M., and Croce, C. M. (2005) miR-15 and miR-16 induce apoptosis by targeting BCL2. *Proc. Natl. Acad. Sci. U. S. A.* **102,** 13944–13949
15. Bommer, G. T., Gerin, I., Feng, Y., Kaczorowski, A. J., Kuick, R., Love, R. E., Zhai, Y., Giordano, T. J., Qin, Z. S., Moore, B. B., MacDougald, O. A., Cho, K. R., and Fearon, E. R. (2007) p53-mediated activation of miRNA34 candidate tumor-suppressor genes. *Curr. Biol.* **17,** 1298–1307
16. Ghisolfi, L., Calastretti, A., Franzi, S., Canti, G., Donnini, M., Capaccioli, S., Nicolin, A., and Bevilacqua, A. (2009) B cell lymphoma (Bcl)-2 protein is the major determinant in bcl-2 adenine-uridine-rich element turnover overcoming HuR activity. *J. Biol. Chem.* **284,** 20946–20955
17. Bakhshi, A., Jensen, J. P., Goldman, Wright, P. J. J., McBride, O. W., Epstein, A. L., and Korsmeyer, S. J. (1985) Cloning the chromosomal breakpoint of t(14;18) human lymphomas: clustering around JH on chromosome 14 and near a transcriptional unit on 18. *Cell* **41,** 899–906
18. Steube, K. G., Jadau, A., Teepe, D., and Drexler, H. G. (1995) Expression of bcl-2 mRNA and protein in leukemia-lymphoma cell lines. *Leukemia* **9,** 1841–1846
19. Robertson, L. E., Plunkett, W., McConnell, K., Keating, M. J., and McDonnell, T. J. (1996) Bcl-2 expression in chronic lymphocytic leukemia and its correlation with the induction of apoptosis and clinical outcome. *Leukemia* **10,** 456–459
20. Pui, C. H., Relling, M. V., and Downing, J. R. (2004) Acute lymphoblastic leukemia. *N. Engl. J. Med.* **350,** 1535–1548
21. Pui, C. H., and Evans, W. E. (2006) Treatment of acute lymphoblastic leukemia. *N. Engl. J. Med.* **354,** 166–178
22. Valerie, I., Brown, V. I., Seif, A. E., Reid, G. S. D., Teachey, D. T., and Grupp, S. A. (2008) Novel molecular and cellular therapeutic targets in acute lymphoblastic leukemia and lymphoproliferative disease. *Immunol. Res.* **42,** 84–105
23. Gaynon, P. S., Qu, R. P., Chappell, R. J., Willoughby, M. L., Tubergen, D. G., Steinherz, P. G., and Trigg, M. E. (1998) Survival after relapse in childhood acute lymphoblastic leukemia: impact of site and time to first relapse—the Children's Cancer Group Experience. *Cancer* **82,** 1387–1395
24. Chessells, J. M. Relapsed lymphoblastic leukaemia in children: a continuing challenge. *Br. J. Haematol.* **102,** 423–433
25. Borgmann, A., von Stackelberg, A., Hartmann, R., Ebell, W., Klingebiel, T., Peters, C., and Henze, G. (2003) Unrelated donor stem cell transplantation compared with chemotherapy for children with acute lymphoblastic leukemia in a second remission: a matched-pair analysis. *Blood* **101,** 3835–3839
26. Pui, C. H., Robison, L. L., and Look, A. T. (2008) Acute lymphoblastic leukaemia. *Lancet* **371,** 1030–1043
27. Porté, S., Crosas, E., Yakovtseva, E., Biosca, J. A., Farrés, J., Fernández, M. R., and Parés, X. (2009) MDR quinone oxidoreductases: the human and yeast zeta-crystallins. *Chem. Biol. Interact.* **178,** 288–294
28. Huang, Q. L., Russell, P., Stone, S. H., and Zigler, J. S., Jr. (1987) ζ-Crystallin, a novel lens protein from the guinea pig. *Curr. Eye Res.* **6,** 725–732
29. Garland. D., Rao, P. V., Del Corso, A., Mura, U., and Zigler, J. S., Jr. (1991) ζ-Crystallin is a major protein in the lens of *Camelus dromedarius*. *Arch. Biochem. Biophys.* **285,** 134–136
30. Duhaiman, A. S., Rabbani, N., AlJafari, A. A., and Alhomida, A. S. (1995) Purification and characterization of ζ-crystallin from the camel lens. *Biochem. Biophys. Res. Commun.* **215,** 632–640
31. Fujii, Y., Kimoto, H., Ishikawa, K., Watanabe, K., Yokota, Y., Nakai, N., and Taketo, A. (2001) Taxon-specific ζ-crystallin in Japanese tree frog (*Hyla japonica*) lens. *J. Biol. Chem.* **276,** 28134–28139
32. Mano, J., Yoon, H., Asada, K., Babiychuk, E., Inzé, D., and Mikami, B. (2000) Crystallization and preliminary X-ray crystallographic analysis of NADPH: azodicarbonyl/quinone oxidoreductase, a plant ζ-crystallin. *Biochim. Biophys. Acta* **1480,** 374–376
33. Kranthi, B. V., Balasubramanian, N., and Rangarajan, P. N. (2006) Isolation of a single-stranded DNA-binding protein from the methylotrophic yeast, *Pichia pastoris* and its identification as ζ crystallin. *Nucleic Acids Res.* **34,** 4060–4068
34. Rodokanaki, A., Holmes, R. K., and Borras, T. (1989) ζ-Crystallin, a novel protein from the guinea pig lens is related to alcohol dehydrogenases. *Gene* **78,** 215–224
35. Rao, P. V., Krishna, C. M., and Zigler, J. S., Jr. (1992) Identification and characterization of the enzymatic activity of ζ-crystallin from guinea pig lens. A novel NADPH:quinone oxidoreductase. *J. Biol. Chem.* **267,** 96–102
36. Rao, P. V., and Zigler, J. S., Jr. (1992) Purification and characterization of ζ-crystallin/quinone reductase from guinea pig liver. *Biochim. Biophys. Acta* **1117,** 315–320
37. Gonzalez, P., Rao, P. V., and Zigler, J. S., Jr. (1993) Molecular cloning and sequencing of ζ-crystallin/quinone reductase cDNA from human liver. *Biochem. Biophys. Res. Commun.* **1191,** 902–907
38. Tang, A., and Curthoys, N. P. (2001) Identification of ζ-crystallin/NADPH:quinone reductase as a renal glutaminase mRNA pH response element-binding protein. *J. Biol. Chem.* **276,** 21375–21380
39. Ibrahim, H., Lee, Y. J., and Curthoys, N. P. (2008) Renal response to metabolic acidosis: role of mRNA stabilization. *Kidney Int.* **73,** 11–18
40. Schroeder, J. M., Liu, W., and Curthoys, N. P. (2003) pH-responsive stabilization of glutamate dehydrogenase mRNA in LLC-PK1-F^+ cells. *Am. J. Physiol. Renal Physiol.* **285,** F258–F265
41. Fernández, M. R., Porté, S., Crosas, E., Barberà, N., Farrés, J., Biosca, J. A., and Parés, X. (2007) Human and yeast ζ-crystallins bind AU-rich elements in RNA. *Cell. Mol. Life Sci.* **64,** 1419–1427

42. Bevilacqua, A., Ghisolfi, L., Franzi, S., Maresca, G., Gherzi, R., Capaccioli, S., Nicolin, A., and Canti, G. (2007) Stabilization of cellular mRNAs and up-regulation of proteins by oligoribonucleotides homologous to the Bcl2 adenine-uridine rich element motif. *Mol. Pharmacol.* **71,** 531–538
43. Amedei, A., Romagnani, C., Benagiano, M., Azzurri, A., Fomia, F., Torrente, F., Plebani, A., D'Elios, M. M., and Del Prete, G. (2001) Preferential Th1 profile of T helper cell responses in X-linked (Bruton's) agammaglobulinemia. *Eur. J. Immunol.* **31,** 1927–1934
44. Cok, S. J., Acton, S. J., Sexton, A. E., and Morrison, A. R. (2004) Identification of RNA-binding proteins in RAW 264.7 cells that recognize a lipopolysaccharide-responsive element in the 3-untranslated region of the murine cyclooxygenase-2 mRNA. *J. Biol. Chem.* **279,** 8196–8205
45. Niranjanakumari, S., Lasda, E., Brazas, R., and Garcia-Blanco, M. A. (2002) Reversible cross-linking combined with immunoprecipitation to study RNA-protein interactions in vivo. *Methods* **26,** 182–190
46. Otake, Y., Soundararajan, S., Sengupta, T. K., Kio, E. A., Smith, J. C., Pineda-Roman, M., Stuart, R. K., Spicer, E. K., and Fernández, D. J. (2007) Over-expression of nucleolin in chronic lymphocytic leukemia cells induces stabilization of bcl-2 mRNA. *Blood* **109,** 9069–9075
47. Ferrando, A. A., Neuberg, D. S., Staunton, J., Loh, M. L., Huard, C., Raimondi, S. C., Behm, F. G., Pui, C. H., Downing, J. R., Gilliland, D. G., Lander, E. S., Golub, T. R., and Look, A. T. (2002) Gene expression signatures define novel oncogenic pathways in T cell acute lymphoblastic leukemia. *Cancer Cell* **1,** 75–87
48. Harrison. C. J., and Foroni, L. (2002) Cytogenetics and molecular genetics of acute lymphoblastic leukemia. *Rev. Clin. Exp. Hematol.* **6,** 91–113
49. Graux, C., Cools, J., Michaux, L., Vandenberghe, P., and Hagemeijer, A. (2006) Cytogenetics and molecular genetics of T-cell acute lymphoblastic leukemia: from thymocyte to lymphoblast. *Leukemia* **20,** 1496–1510
50. Rich, B. E., Campos-Torres, J., Tepper, R. I., Moreadith, R. W., and Leder, P. (1993) Cutaneous lymphoproliferation and lymphomas in interleukin 7 transgenic mice. *J. Exp. Med.* **177,** 305–316
51. Karawajew, L., Ruppert, V., Wuchter, C., Kösser, A., Schrappe, M., Dörken, B., and Ludwig, W. D. (2000) Inhibition of in vitro spontaneous apoptosis by IL-7 correlates with bcl-2 up-regulation, cortical/mature immunophenotype, and better early cytoreduction of childhood T-cell acute lymphoblastic leukemia. *Blood* **96,** 297–306
52. Barata, J. T., Cardoso, A. A., Nadler, L. M., and Boussiotis, V. A. (2001) Interleukin-7 promotes survival and cell cycle progression of T-cell acute lymphoblastic leukemia cells by down-regulating the cyclin-dependent kinase inhibitor p27(kip1). *Blood* **98,** 1524–1531
53. Gala, J. L., Vermylen, C., Cornu, G., Ferrant, A., Michaux, J. L., Philippe, M., and Martiat, P. (1994) High expression of bcl-2 is the rule in acute lymphoblastic leukemia, except in Burkitt subtype at presentation, and is not correlated with the prognosis. *Ann. Hematol.* **69,** 17–24
54. Abraham, R. T., and Weiss, A. (2004) Jurkat T cells and development of the T-cell receptor signaling paradigm. *Nat. Rev. Immunol.* **4,** 301–308

Received for publication July 6, 2009.
Accepted for publication December 23, 2009.